

Application of the Proper Orthogonal Decomposition to Turbulent Czochralski Convective Flows

S Rahal¹, P Cerisier² and H Azuma³

¹ Department of Mechanical Engineering, University of Batna, Rue Boukhrouf Mohamed el Hadi, 05000 Batna, ALGERIA.

² IUSTI - CNRS UMR 6595, Polytech'Marseille, Technopôle de Château-Gombert, 5 rue Enrico Fermi, 13453, Marseille Cedex 13, FRANCE.

³ Department of Aerospace Engineering, Osaka Prefecture University, Gakuen-cho 1-1, Sakai, Osaka 599-8531, JAPAN.

Abstract. The aim of this work is to study the general aspects of the convective flow instabilities in a simulated Czochralski system. We considered the influence of the buoyancy and crystal rotation. Velocity fields, obtained by an ultrasonic technique, the corresponding 2D Fourier spectra and a correlation function, have been used. Steady, quasi-periodic and turbulent flows, are successively recognized, as the Reynolds number was increased, for a fixed Rayleigh number. The orthogonal decomposition method was applied and the numbers of modes, involved in the dynamics of turbulent flows, calculated. As far as we know, this method has been used for the first time to study the Czochralski convective flows. This method provides also information on the most important modes and allows simple theoretical models to be established. The large rotation rates of the crystal were found to stabilize the flow, and conversely the temperature gradients destabilize the flow. Indeed, the increase of the rotation effects reduces the number of involved modes and oscillations, and conversely, as expected, the increase of the buoyancy effects induces more modes to be involved in the dynamics. Thus, the flow oscillations can be reduced either by increasing the crystal rotation rate to the adequate value, as shown in this study or by imposing a magnetic field.

1. Introduction

Although several methods have been used to manufacture silicon single crystals, the so-called Czochralski (Cz) crystal puller method is widely used for industrial production. This fact comes from the ability of the Cz method to meet the stringent requirements for purity and crystallographic perfection. A comprehensive introduction and review of the research carried out on this flow, prior to 1997, can be found in [1]. More recently, other papers dealing with the Cz convective system have been published [2-4]. These papers were mainly devoted to the numerical modelling of the flow instabilities and the application of a magnetic field to suppress the flow oscillations.

The flow structure in a Czochralski crucible during silicon crystal growth influences the quality of the grown crystals [5]. Indeed, the flow oscillations, caused by the flow of the melt, are known to have an especially strong influence upon microdefects and striations which appear in the final crystal and which are detrimental to the quality of semi-conductor devices made from it [6]. Thus, a more complete understanding of the transport phenomena and the fluid flow in silicon melts is essential.

Recently, much effort has been devoted to producing large-sized crystals to increase the productivity of semiconductor industry. Since the size of the Czochralski crucible has to be large, the assumption of a laminar flow may not be valid. Indeed, the large values of Reynolds (Re) and Rayleigh (Ra) numbers for such extended systems imply that the fluid motions may be turbulent.

Once a turbulent state is recognized, it is interesting to measure at least the number of modes involved in the turbulent dynamics. For that purpose, the Karhunen-Loeve (KL) decomposition [7] has been applied to experimental [8, 9] and numerical data sets [10, 11]. More recently, it has been used to analyse the flow structures in a ventilated room [12] and has been applied to data sets of internal combustion engine flows [13]. This method is useful not only in estimating the number of the degrees of freedom of a dynamic system, but allows also theoretical models of the systems under study to be established [14]. This method has been applied to few experimental data sets because of a lack of a suitable measurement method that can provide spatio-temporal information with sufficient resolutions. Now, we can use the Ultrasonic Velocity Profile (UVP) technique [15] which allows obtaining a suitable spatio-temporal velocity field.

As far as we know, no experimental work has been carried out to study the influence of the rotation rate (Reynolds number) and the gradient of temperature (Rayleigh number) on the Cz flow instabilities, using the 2D Fourier spectra and the correlation function to recognize the various flow states, and the orthogonal decomposition method to estimate the number of degrees of freedom (dimension) of the turbulent regimes. The use of such methods allows a more understanding of the Cz flow instabilities and might be useful in giving us the means to suppress or control its oscillations.

Consequently this paper deals with such problems using velocity fields, obtained by the UVP technique. The paper is organized as follows, in section 2, the experimental setup and the UVP technique are briefly described. In section 3, the different methods, used to analyze the Cz flow, are presented; the results are presented and discussed in section 4. In section 5, some conclusions are given.

2. Experimental procedure

The experimental setup, as shown in Figure 1, consisted of a simulated crucible (1) made of Pyrex glass of 10 cm inner diameter and 10 cm height. A simulated crystal (2) of 3 cm diameter made of brass. The crucible (1) was filled with 2 centistokes silicone oil (Prandtl number, $Pr = 28$ at $T = 25$ °C) as a model liquid (3).

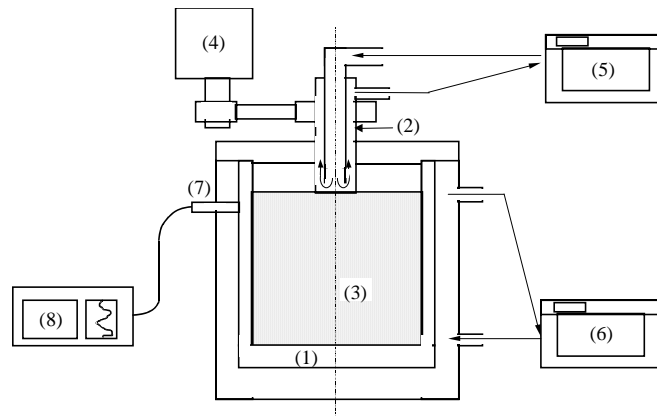


Figure 1. Schematic of the experimental set-up, (1) simulated crucible, (2) simulated crystal, (3) silicone oil, (4) Motor to rotate the simulated crystal, (5) and (6) temperature-regulated baths, (7) UVP sensor, (8) UVP monitor.

The simulated crystal (2) was rotated by a motor (4). The temperature gradient between the crucible and the crystal was obtained by circulating cold and hot water flows respectively coming from two temperature-regulated baths (5, 6). The flows were visualized in the vertical median plane using a light sheet. Powdered ferrite was used as a tracer.

In many studies, the number of simultaneous measurements is limited by the number of sensors and/or data acquisition channels. To overcome this problem, we used the UVP method [15], which allowed the instantaneous measurements of velocity profiles. This method uses the pulsed echography

of an ultrasound. An ultrasound pulse is emitted from a transducer along the measurement line (the diameter of the crucible), and the same transducer receives the echo reflected back from particles scattered in the fluid. The position information is given by the time elapsing between the pulse emission and the echo reception, and velocity information is obtained from the Doppler shift in the frequency at each instant. The UVP sensor (7) was set 1 cm below the liquid upper surface, and in contact with the outer wall of the crucible.

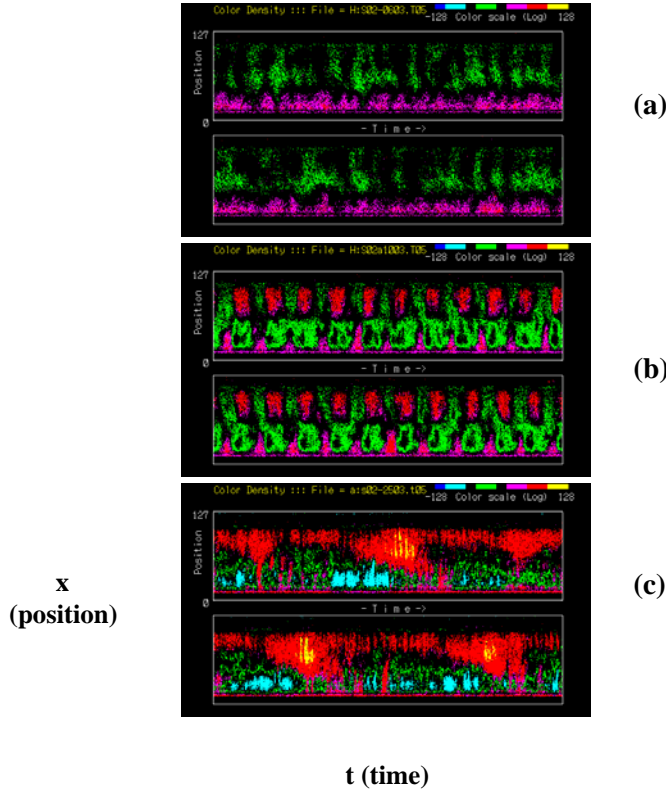


Figure 2. Velocity profiles for a fixed $Ra (=10^7)$.
 (a) steady state ($Re = 7.1 \times 10^2$),
 (b) quasi-periodic state ($Re = 1.2 \times 10^3$),
 (c) turbulent state ($Re = 2.9 \times 10^3$).

Figure 2 shows examples of UVP fields. There are 128 measurement points per profile and one experimental run consists of 1024 temporal profiles that are successively collected (the measurement time is 554 s for the data in Figure 2). The speed and direction of the flow are color-coded. The flow moving towards the probe is green to blue, and red to yellow, away from the probe. These fields were used as the basis on which the analysis has been conducted.

The flow was studied as a function of the relevant physical parameters in the Czochralski flow, namely, the Rayleigh number, $Ra = g\beta\Delta T R_{\text{cru}}^3/\nu\kappa$ and the Reynolds number, $Re = \Omega R_{\text{cry}}^2/\nu$, where R_{cry} and R_{cru} are the radius of the crystal and the crucible respectively; ΔT is the difference of temperature applied between the crucible and the crystal; β is the volumetric coefficient of thermal expansion, ν is the kinematic viscosity, κ is the thermal diffusivity, Ω is the angular velocity of the crystal, and g is the gravity.

3. Analysis methods

The spatio-temporal nature of the flow is clearly obtained and displayed on the UVP data (Figure 2). However, to further understand the phenomena involved, we used the following methods.

3.1. Fourier Spectrum

The UVP data can be analyzed by a 2D Fourier transform to generate a 2D spectrum on the wavenumber ($k = 0$ to 127) and frequency ($f = 0$ to 511 Hz). The evolution of the flow through its velocity fields can then be studied using the corresponding frequency-wavenumber spectra. This method is very useful because it allows one to gather on the same figure the temporal modes (through the frequency of oscillation, f , axis corresponding to the time axis in the velocity profile) and spatial modes (through the wavenumber, k , axis corresponding to the position axis in the velocity profile).

3.2. Correlation function

We have also computed the temporal correlation function, defined as:

$$C(t) = \frac{\left\langle [v(x,t) - \langle v \rangle] [v(x,0) - \langle v \rangle] \right\rangle}{\left\langle v^2 \right\rangle} \quad (1)$$

where $v(x, t)$ and $v(x, 0)$ are the values of the velocity at the same position measured at different times and $\langle \rangle$ denotes an average.

3.3. Karhunen-Loève (KL) decomposition

As the KL decomposition applied to dynamic systems has been described in detail [7], we will restrict ourselves here to describing the overall concept.

The field to be decomposed using the KL method is a velocity field $v(x, t)$ obtained by UVP. Each data set is composed of 128×1024 velocities in a matrix form.

Consider a data set

$$\{v_i, i = 1, \dots, n\} \quad (2)$$

where each v_i is an m -vector

$$v_i = (v_{1i}, \dots, v_{mi})^T \quad (3)$$

where $n = 1024$ and $m = 128$ in this case.

The principle of the method is to find a set of vectors that forms a basis. The resolution leads to an eigenvalue problem for the Φ 's :

$$C\Phi_j = \lambda_j\Phi_j \quad (4)$$

where

$$C = \left\langle v_i v_i^T \right\rangle \quad (5)$$

is the ensemble averaged covariance matrix, and the Φ 's are called the empirical eigenfunctions or coherent structures. C is a $m \times m$ (128×128) symmetrical non-negative matrix, and consequently determines a complete set of orthogonal eigenvectors, and real, non-negative, eigenvalues. These eigenvalues can be ordered, thus:

$$\lambda_1 \geq \lambda_2 \geq \lambda_3 \dots \geq \lambda_m \quad (6)$$

where λ_j is the energy of mode j and

$$E = \sum_{j=1}^m \lambda_j \quad (7)$$

is the total energy of the system.

Once the Φ 's are determined by finding the eigenvectors of C , the a_{ij} coefficient can be found by projecting the data vectors onto each eigenvector in turn:

$$a_{ij} = (v_i, \Phi_j) \quad (8)$$

These coefficients (a_{ij}) are referred to as "reconstruction coefficients". To study how the energy of the flow is distributed among the modes, we have defined the quantity:

$$R(p) = \sum_{j=1}^p \frac{\lambda_j}{E} \quad (9)$$

which is the percentage of the energy contained in the first p modes. In order to estimate the dimension of a flow, we used the KL dimension, D_{kl} , which is the number of modes capturing 90 % of the total energy of the flow [16].

4. Results and discussion

In the Cz flow, the most important driving forces are i) the centrifugal force due to the crystal rotation (Figure 3(a)); and ii) the buoyancy force due to the temperature gradient (Figure 3(b)). As a result of the combination of the flows induced by these forces and other forces such as the Marangoni convection, the flow behaves in a very complex manner in the crucible.

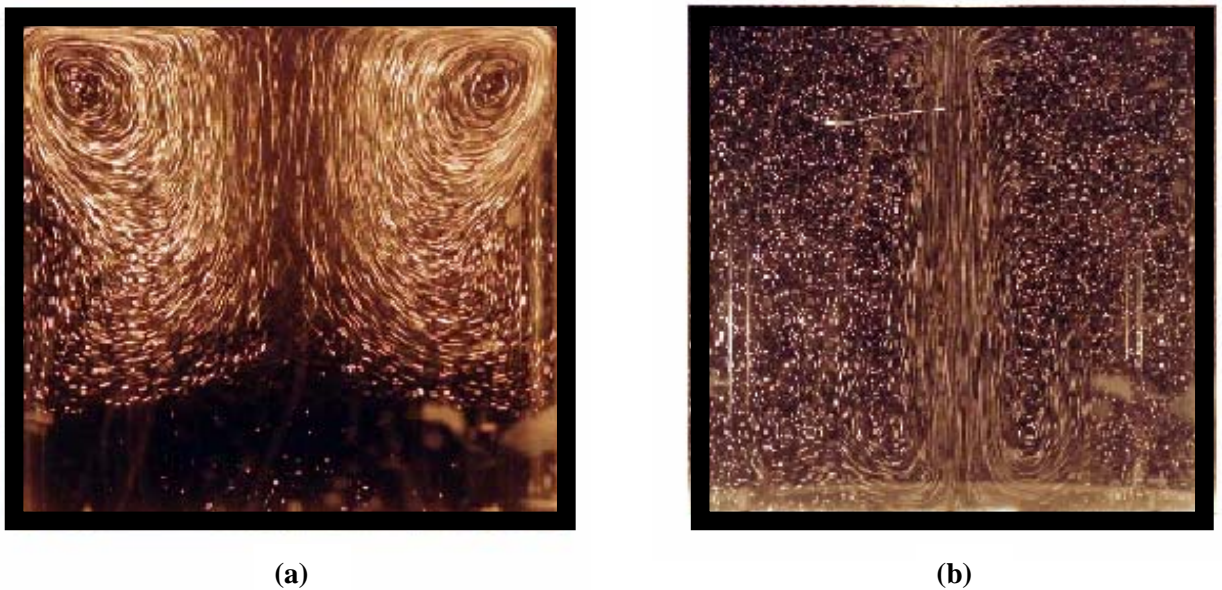


Figure 3. Observed patterns, taken with 1 second exposure time, in 2 cSt silicone oil.

(a) $Ra = 0$, $Re = 5.9 \times 10^2$; (b) $Ra = 10^7$, $Re = 0$.

Velocity profiles representing the observed states for different values of Re for a fixed $Ra (= 10^7)$ are shown in Figure 2. Figure 2(a) corresponds to a steady state without temporal variation of the velocity, Figure 2(b) corresponds to an oscillatory quasi-periodic state and Figure 2(c) corresponds to a turbulent state without periodicity in either space or in time.

The application of 2D Fourier transforms to the velocity fields of Figure 2 gives the spectra shown in Figure 4. Indeed, Figure 4(a) corresponds to a steady state without any oscillations of the velocity; Figure 4(b) shows a spectrum corresponding to an oscillatory quasi-periodic state; whereas the spectrum of Figure 4(c) corresponds to a turbulent state with large dispersions both in the frequency of oscillation (f) and the wavenumber (k), indicating the presence of a large number of temporal and spatial modes, which is the characteristic of a turbulent flow.

So the evolution of these Fourier spectra as a function of Re for a fixed $Ra (= 10^7)$ clearly shows the transition between states leading finally to a turbulent one.

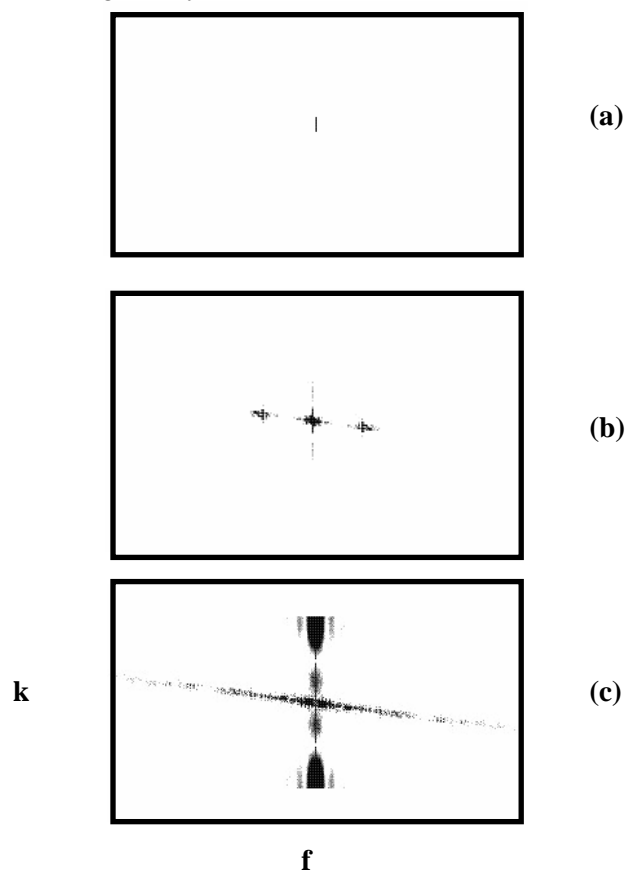


Figure 4. 2D power spectra of the velocity profiles of figure 2. Horizontal and vertical axes are the frequency (f) and wavenumber (k) axes, respectively. $Ra = 10^7$.

- (a) steady state ($Re = 7.1 \times 10^2$),
- (b) quasi-periodic state ($Re = 1.2 \times 10^3$),
- (c) turbulent state ($Re = 2.9 \times 10^3$).

The correlation function shown in Figure 5, corresponding to the velocity profile at $Re = 2.9 \times 10^3$, was observed to globally decrease and is expected to vanish for a longer period of time, that is, indicating a loss of correlation of the system which is a characteristic of a turbulent state.

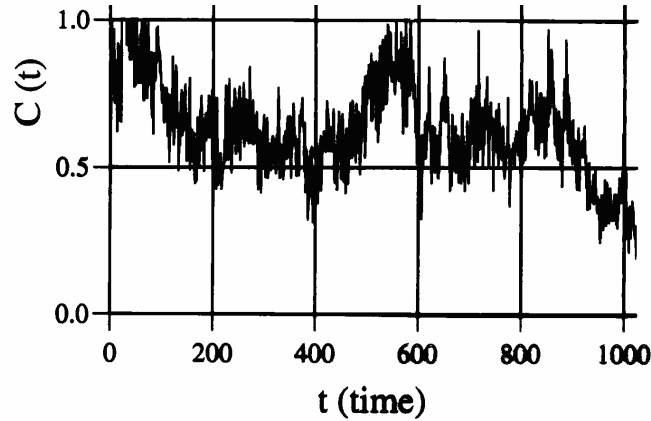


Figure 5. Temporal correlation function of the velocity profile corresponding to the turbulent state ($Re = 2.9 \cdot 10^3$).

Once a turbulent flow is recognized, it is interesting to estimate the number of modes that may produce such behaviour. For this purpose, we applied the KL decomposition. The cumulative energy $R(p)$ versus p is shown in Figure 6 for different values of Re and Ra . Clearly, $R(p)$ reaches 90 % of the total energy at lower p values as Re is increased.

The opposite was found with increasing Ra . This means that D_{kl} decreases as Re is increased ($D_{kl} = 38$ for $Re = 1.8 \times 10^3$ and $D_{kl} = 4$ for $Re = 2.9 \times 10^3$ for $Ra = 10^7$), and increases with Ra ($D_{kl} = 38$ for $Ra = 10^7$ and $D_{kl} = 57$ for $Ra = 7.2 \times 10^7$ for $Re = 2.9 \times 10^3$). We can conclude that the rotation effects are stabilizing the flow, and the gradients of temperature have a destabilizing role. Indeed, more modes and oscillations are involved when the buoyancy effects (Ra number) are increased.

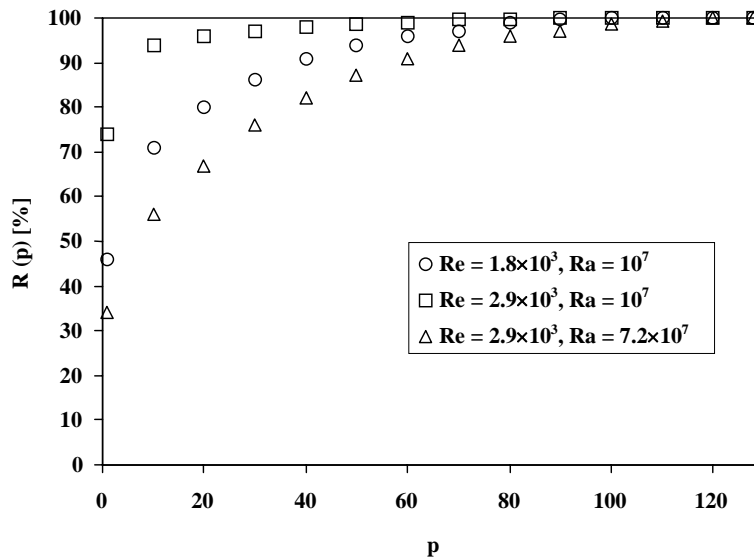


Figure 6. The cumulative energy $R(p)$ versus p for various Re and Ra .

5. Conclusions

The proper orthogonal decomposition is a fruitful tool to study the Czochralski flow. In this preliminary study of the transition mechanisms between states in a model of this flow, steady, quasi-periodic and turbulent flows were successively observed as the Reynolds number was increased, for a

fixed Rayleigh number. The different states were recognized using the velocity profiles, their 2D Fourier spectra and a correlation function.

The number of modes involved in the dynamics was estimated using the KL decomposition. This method provides also information on the most important modes. The large rotation rates of the crystal were found to stabilize the flow, and conversely the temperature gradients destabilized the flow.

REFERENCES

- [1] Prasad V, Zhang H and Anselmo A P 1997 Transport Phenomena in Czochralski Growth Process *Advances in Heat Transfer* ed J P Hartnett, T F Irvine, Y I Cho and G A Greene, **30** (Academic Press) pp 313 - 435.
- [2] Miller W, Rehse U and Bottcher K 1999 Melt convection in a Czochralski crucible *Crystal research technology* **34** (4) 481 - 89.
- [3] Voigt A, Weichmann C, Nitschkowski J, Dormberger E and Holz R 2003 Transient and quasi-stationary simulation of heat and mass transfer in Czochralski silicon crystal growth *Crystal research technology* **38** (6) 499-505.
- [4] Li Y R, Ruan D F, Imaishi N, Wu S Y, Peng L and Zeng D L 2003 Global simulation of a silicon Czochralski furnace in an axial magnetic field *Int. J. Heat and Mass Transfer* **46** (15) 2887 - 98.
- [5] Hirata A, Okano Y, Yakushiji K and Harrison B 1992 Czochralski Process *Advances in Transport Processes* ed A S Mujumdar and R A Mashelkar **8** (Elsevier) pp 435 -504.
- [6] Kanda T, Hourai M, Miki S, Shigematsu T, Tomokage H, Miyano T, Morita H and Shintani A 1996 Influence of Melt-temperature Fluctuations on Striation Formation in Large-Scale Czochralski Si Growth Systems *J. Crystal Growth* **166** 663 - 68.
- [7] Berkooz G, Holmes P and Lumley J L 1993 The proper orthogonal decomposition in the analysis of turbulent flow *Annu. Rev. Fluid Mech.* **25** 115-159.
- [8] Broomhead D S and King G P 1996 Extracting qualitative dynamics from experimental data *Physica D* **20** 217 - 36.
- [9] Glezer A, Kadioglu Z and Pearlstein A J 1989 Development of an extended proper orthogonal decomposition and its application to a time periodically forced plane mixing layer *Phys. Fluids A* **1**(8) 1363 - 73.
- [10] Sirovich L, Ball K S and Keefe L R 1990 Plane waves and structures in turbulent channel flow *Phys. Fluids A* **2**(12) 2217 - 26.
- [11] Webber G A, Handler R A and Sirovich L 1997 The Karhunen-Loeve decomposition of minimal channel flow *Phys. Fluids* **9** (4) 1054- 63.
- [12] Pedersen J and Meyer K 2002 POD analysis of flow structures in a scale model of a ventilated room *Experiments in Fluids* **33** (6) 940 - 49.
- [13] Fogleman M, Lumley J, Rempfer D and Haworth D 2004 Application of the proper orthogonal decomposition to datasets of internal combustion engine flows *J. Turbulence* **5** 1 - 18.
- [14] Sirovich L and Rodriguez J D 1987 Coherent structures and chaos: A model problem *Phys. Lett. A* **120** 5 - 8.
- [15] Takeda Y 1991 Development of an Ultrasound Velocity Profile Monitor *Nucl. Eng. Des.* **126** 277 - 84.
- [16] Sirovich L 1991 Empirical eigenfunctions and low dimensional systems *New Perspectives in Turbulence* (Springer-Verlag) pp139-163.